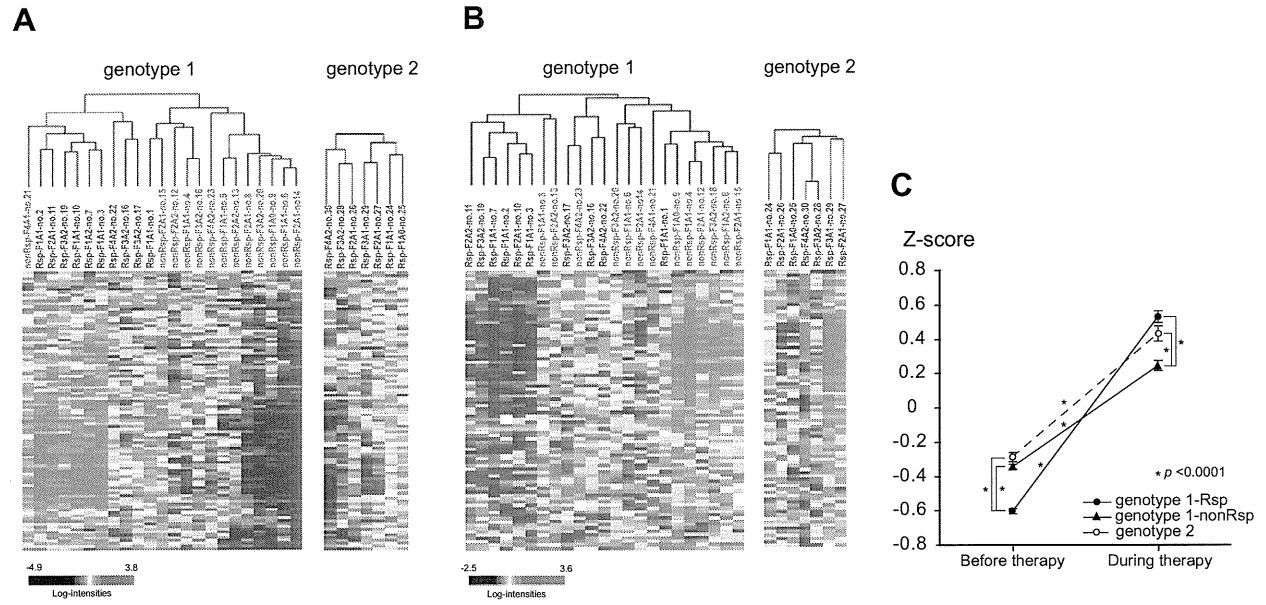

Fig. 1. (A) Hierarchical clustering of expression in genotype 1 and genotype 2 patients during treatment according to fold induction of IRSGs. (B) Hierarchical clustering of expression in genotype 1 and genotype 2 patients before treatment. (C) Serial changes in standardized expression values (*Z*-score) of IRSGs from genotype 1-Rsp, genotype 1-nonRsp, and genotype 2 patients before and during treatment.

Statistical and pathway analysis of gene chip data

Statistical analysis and hierarchical clustering were performed by BRB-ArrayTools (http://linus.nci.nih.gov/BRB-ArrayTools.htm). A class comparison tool based on univariate or paired *t*-tests was used to find differentially expressed genes (p <0.005). To confirm statistical significance, 2000 random permutations were performed, and all of the *t*-tests were re-computed for each gene. The gene set comparison was analyzed using the BioCarta and the KEGG pathway data bases. The Fisher and Kolmogorov–Smirnov tests were performed for statistical evaluation (p <0.005) (BRB-ArrayTools). Functional ontology enrichment analysis was performed to compare the Gene Ontology (GO) process distribution of differentially expressed genes (p <0.05) using MetaCore™ (GeneGo, St. Joseph, MI, USA).

For the comparison of standardized expression values among different pathway groups, standard units (*Z*-score) of each gene expression value were calculated as:

$$Z_i = \frac{X_i - X_m}{S}$$

where X_i is the raw expression value, X_m is the mean of the expression values in the pathway, and S is the standard deviation of the expression values.

The standard units in each pathway were expressed as mean ± SEM. A *P*-value of less than 0.05 was considered significant. Multivariate analysis was performed using a logistic regression model with a stepwise method using JMP7 for Windows (SAS Institute, Cary, NC, USA).

Quantitative real-time detection (RTD)-PCR

We performed quantitative real-time detection PCR (RTD)-PCR using TaqMan Universal Master Mix (PE Applied Biosystems, CA). Primer pairs and probes for Mx1, IFI44 and IFITM1, and GAPDH were obtained from TaqMan assay reagents library (Applied Biosystems, CA).

Results

Serial changes in HCV-RNA after initiation of IFN-α 2b and Rib combination therapy

Serial changes in HCV-RNA were monitored at 48 h, 2 weeks, and 24 weeks after the initiation of therapy (Table 1). The biphasic viral decline after the initiation of IFN therapy has been characterized [14,15,18]. We calculated the first phase decline by comparing viral load before therapy and after 48 h, and the second phase decline by comparing viral load after 48 h and 2 weeks (Table 1) [14,15,18]. Both the first and the second phase declines could be associated with treatment outcome and interestingly, viral responders (Rsp) who achieved SVR or TR showed more than a 1-log drop of first phase decline (Log/24 h) and more than a 0.3-log drop of second phase decline (Log/w) (Table 1). In contrast, non-responders (nonRsp) who exhibited NR failed to meet the criteria. The first phase decline of Rsp and nonRsp were 1.38 ± 0.65 log/24 h and 0.77 ± 0.44 log/24 h (p = 0.005), respectively. The second phase decline of Rsp and nonRsp were 0.71 ± 0.34 log/w and 0.11 ± 0.34 log/w (p = 0.0001), respectively. Therefore, the classification of Rsp or nonRsp according to the treatment outcome might be feasible based on the viral kinetic responses to IFN. All but one patient infected with genotype 2 HCV eliminated the virus within 2 weeks. There were no significant differences in the degree of histological activity or staging, nor in the sex, age, or alanine aminotransferase (ALT) level among these patients (Table 1). The amount of HCV-RNA was significantly lower in genotype 2 patients (4.06 ± 0.32 log IU/ml) than in genotype 1 patients (5.70 ± 1.10 log IU/ml) (Table 1).

Identification of IFN-α 2b plus Rib-induced genes in the livers of patients with chronic hepatitis C infection

To identify the genes induced in the liver by combination treatment with IFN-α 2b plus Rib, the gene expression profiles from samples taken around 1 week before and 1 week after initiation of therapy were compared. The pairwise *t*-test comparison showed that 798 genes were up-regulated and 220 genes were down-regulated significantly (p <0.005). The 100 most up-regulated genes according to p values were selected; these are listed in Supplementary Table 1. Many of the interferon-stimulated

genes (ISGs), such as Myxovirus (influenza virus) resistance 1 (MX), 2′,5′-oligoadenylate synthetase (OAS), chemokine (C–C motif) ligand 8 (CCL8), and interferon alpha-inducible protein 27 (IFI 27), were significantly induced (Supplementary Table 1). We designated these genes as *IFN and Rib-stimulated genes* (IRSGs) and analyzed them further.

Hepatic gene expression and responsiveness to IFN-α 2b and Rib combination therapy

To investigate the relationship between hepatic gene expression and responsiveness to treatment, we applied nonsupervised learning methods, hierarchical clustering analysis using all the expressed genes ($n = 34,988$) from samples taken before and 1 week after initiation of therapy. While hierarchical clustering analysis did not form clusters when done for all patients, it formed two clusters – Rsp and nonRsp – when performed within genotype 1 patient (data not shown).

Fold changes in expression in the 100 most up-regulated IRSGs, before and during therapy, were calculated and subjected to hierarchical clustering, and this clearly differentiated Rsp, which exhibited higher IRSGs induction, from nonRsp, as shown in Fig. 1A and Supplementary Table 1. Despite the rapid virus decline in genotype 2 patients, IRSG induction was not so evident in these patients.

Unexpectedly, the hierarchical clustering of IRSG expression in samples taken before treatment showed a reverse pattern of gene expression (Fig. 2B): IRSG induction was significantly higher in nonRsp than in Rsp. Upon treatment, the expression of IRSGs was more induced in Rsp than in nonRsp (Fig. 1C).

The findings were confirmed in patients who were administered Peg-IFN-α 2b and Rib combination therapy (Table 2). IRSG expression was induced in CH-C infected livers and substantially up-regulated in nonRsp compared with Rsp (Supplementary Fig. 1). Multivariate logistic analysis including age, sex, fibrosis stage, activity, HCV-RNA, genotype, treatment regime, ALT and

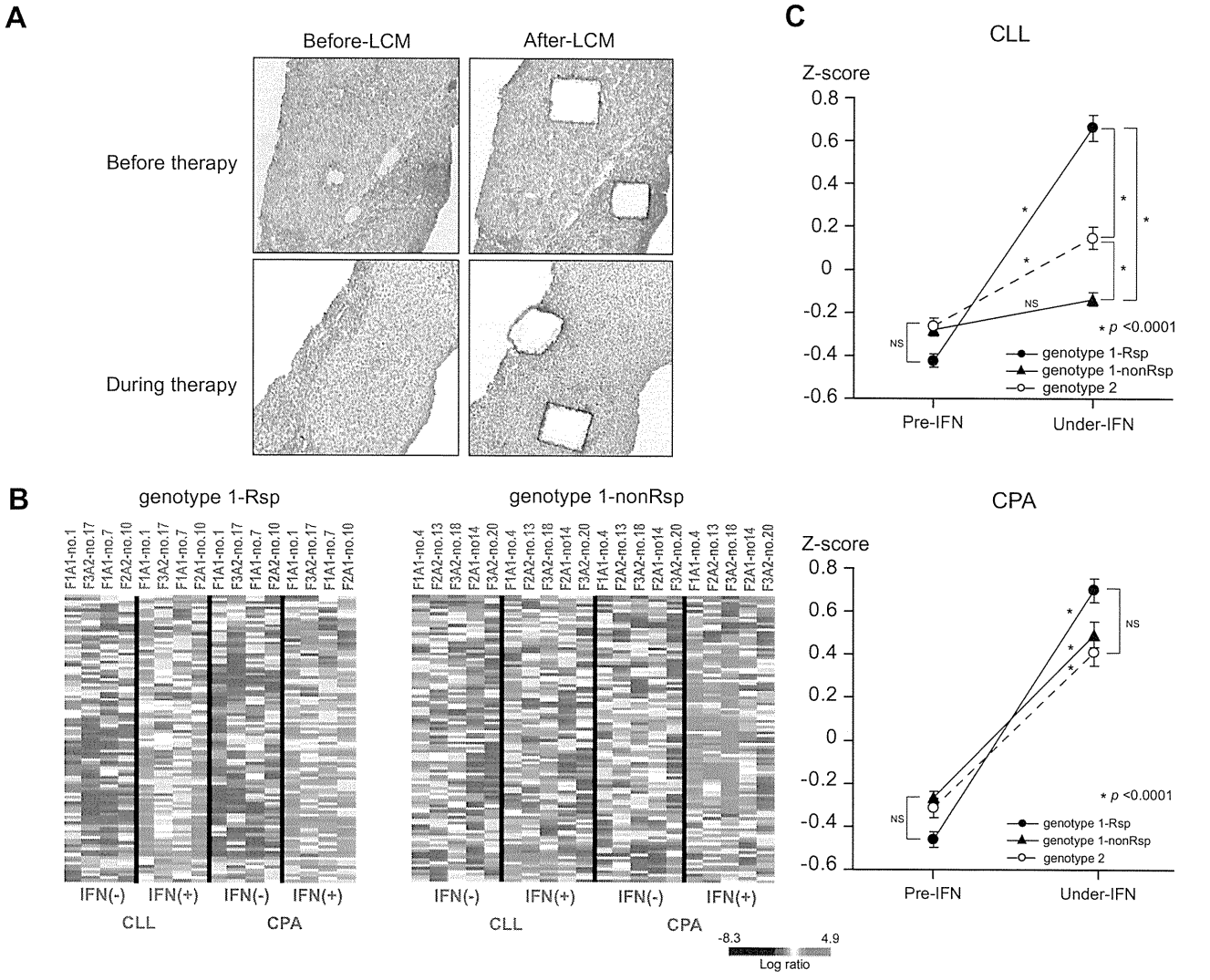

Fig. 2. (A) LCM of liver biopsy samples before and during treatment. (B) Heat map of gene expression of IRSGs in CLL and CPA before and during treatment. (C) Serial changes in standardized expression values (Z-score) of IRSGs in CLL and CPA from genotype 1-Rsp, genotype 1-nonRsp, and genotype 2 patients before and during treatment.

expression pattern of IRSGs (up or down) of the 50 patients before treatment showed that genotype 2 (p <0.0001, Odds = 4×10^7) and down-regulated IRSGs (p <0.0001, Odds = 71.2) are significant variables associated with SVR.

Gene expression analysis in cells in liver lobules (CLL) and portal area (CPA)

To explore these findings in more detail, we examined the gene expression profiles of CLL and CPA that had been isolated separately from whole liver biopsy specimens of 12 patients, using the LCM method before and during treatment (Fig. 2A). The representative differentially expressed genes between CLL and CPA are shown in Supplementary Tables 2-1 and 2-2. In CLL, liver-specific proteins and enzymes, such as cytochrome P450, apolipoprotein, and transferrin, were all expressed. In CPA, cytokines, chemokines and lymphocyte surface markers, such as chemokine (C–X–C motif) receptor 4, interleukin-7 receptor and CD83 antigen, were all expressed (Supplementary Tables 2-1 and 2-2). The results confirmed our previous speculation that cells from the lobular area were mostly of hepatocyte origin and that those from the portal area were mostly of liver-infiltrating lymphocyte origin [11,19].

IRSG expression in CLL and CPA from genotype 1-Rsp and non-Rsp is shown in Fig. 2B. In genotype 1-Rsp, IRSG expression was significantly induced in both CLL and CPA by the treatment (Fig. 2B and C). On the other hand, in genotype 1-nonRsp and genotype 2, IRSG induction was impaired especially in CLL, while

Table 3. Up- and down-regulated pathways by gene set comparison between Rsp and nonRsp of genotype 1 patients before therapy (BRB-array tool).

Pathway	No. of genes	LS p value	KS p value	Representative Genes	Mean probe intensity of representative genes		
					Rsp (n = 20)	nonRsp (n = 23)	Normal (n = 10)
Up-regulated in slow viral drop							
IFN alpha signaling pathway	21	0.00001	0.00300	STAT1	1608	3117	686
				IRF9	1249	1842	614
				IFNAR2	1892	1988	903
Apoptotic Signaling in Response to DNA Damage	55	0.00001	0.07974	CASP3	675	870	426
				CASP7	1165	1510	1264
				CASP9	355	403	264
				TP53	1465	1797	1028
Toll-like receptor signaling pathway	150	0.00006	0.06659	CXCL10	1922	3979	193
				CXCL11	176	321	51
				MYD88	1022	1372	723
				TIRAP	582	722	447
Wnt signal pathway	55	0.00009	0.16058	EIF2AK2	664	1190	484
				CCND1	2439	3558	1162
				APC	143	186	154
				PIK3R1	1570	1906	682
Antigen processing and presentation	139	0.00117	0.00091	TAP2	169	317	93
				HLA-A	11005	14726	6221
				HLA-B	13144	17942	6823
				HLA-C	1937	3993	783
Jak-STAT signaling pathway	220	0.00180	0.13154	STAT2	716	1065	274
				IL28RA	390	544	204
				IL10RB	398	506	338
Down-regulated in slow viral drop							
Metabolism of xenobiotics by cytochrome P450	98	0.00018	0.00082	CYP3A4	15219	10118	19256
				CYP2E1	29129	24549	30929
				AKR1C4	6126	4898	6671
Fatty acid metabolism	88	0.00480	0.05373	ACADL	826	687	785
				ALDH2	18325	16337	21844
				HSD17B4	9619	8807	10653
				ACAD11	6858	6238	8279
				ACOX1	6988	5862	8279

No. of genes, the number of genes comprising the pathway, Rsp, viral responder, patients with SVR or TR; nonRsp, non-viral responder; patients with NR.

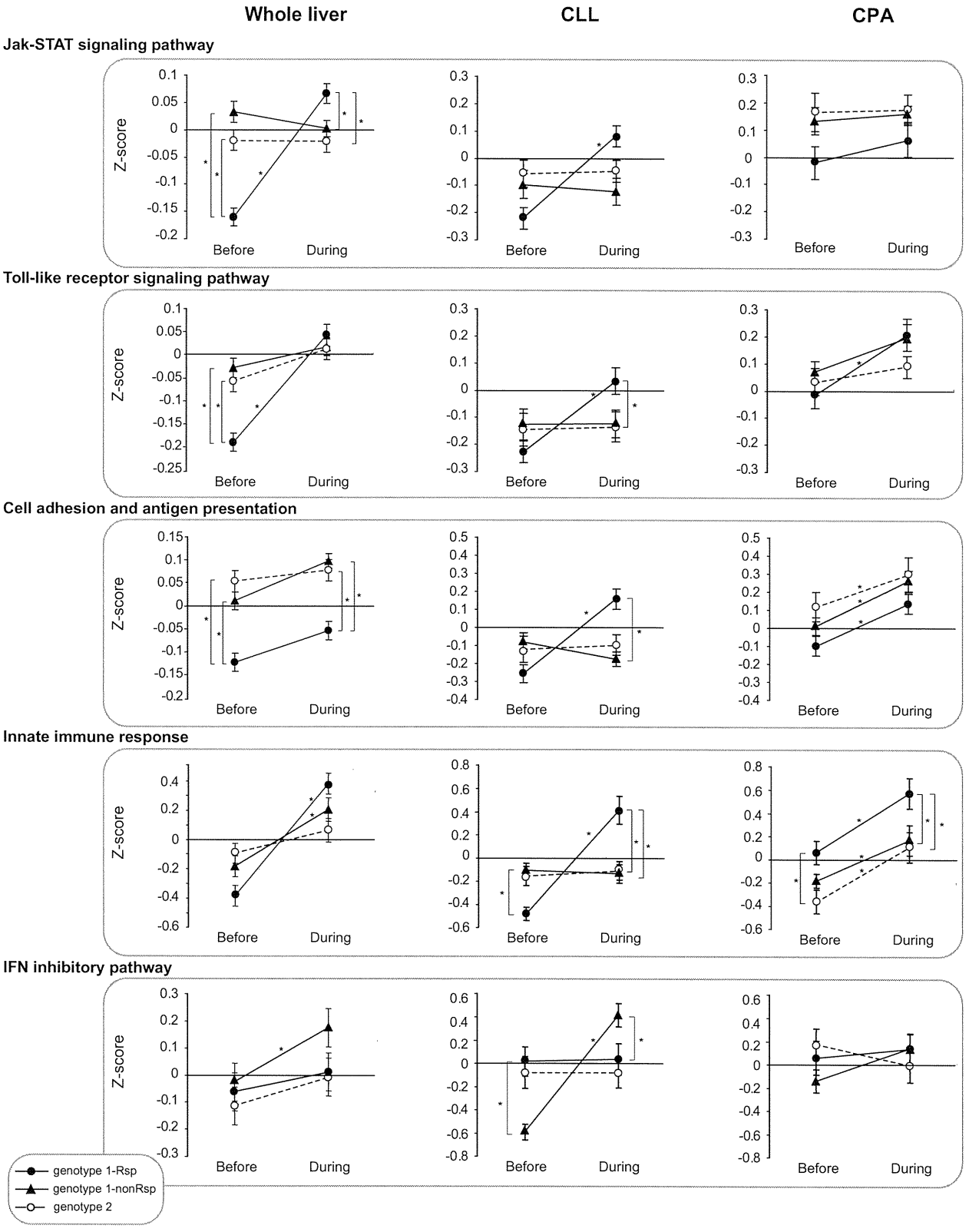

Fig. 3. Serial changes in standardized expression values (Z-score) of differentially expressed pathways from genotype 1-Rsp, genotype 1-nonRsp, and genotype 2 patients before and during treatment in whole liver, CLL, and CPA.

it was nearly preserved in CPA from three of five patients (Fig. 2B and C). Thus, IRSG induction in CLL could play an essential role in the eradication of the virus in genotype 1 CH-C patients.

Pathway analysis of gene expression in the livers of genotype 1-Rsp, genotype 1-nonRsp and genotype 2

To explore which signaling pathway contributed to the impaired IRSG induction, pathway comparisons between genotype 1-Rsp ($n = 20$) and genotype 1-nonRsp ($n = 23$) before treatment were performed (Table 3). Gene set comparison was analyzed based on the database of BioCarta and KEGG pathways. The Fisher and Kolmogorov–Smirnov tests were performed for statistical evaluation ($p < 0.005$) (BRB-ArrayTools). The mean probe intensities of representative genes in individual pathways are shown in Table 3. In genotype 1-nonRsp, the signaling pathways of IFN-α, apoptosis, and many of the immune pathways, such as those involved in antigen presentation, and the toll-like receptor (TRL) and Jak-STAT signaling pathways, were generally expressed at significantly higher levels before treatment than genotype 1-Rsp (Table 3 and Fig. 3). During treatment, the immune pathways were significantly up-regulated in genotype 1-Rsp, while they were not up-regulated in genotype 1-nonRsp and genotype 2 (Fig. 3, whole liver). When the CLL and CPA were analyzed separately, significant induction of these pathways was observed in CLL of genotype 1-Rsp but not of genotype 1-nonRsp and genotype 2 (Fig. 3, CLL). However, similar induction patterns were observed in CPA among genotype 1-Rsp, genotype1-nonRsp, and genotype 2 patients (Fig. 3, CPA). Thus, these immune pathways should be activated in CLL for the elimination of virus.

We then evaluated the extent of the innate immune response to treatment. The expression of 10 innate immune response genes was strongly induced in CLL from patients of genotype 1-Rsp but not from genotype 1-nonRsp and genotype 2 patients, although these genes were similarly induced in CPA among these patients (Supplementary Table 3 and Fig. 3).

To examine which signaling pathways were differentially induced during treatment, we utilized MetaCore™. MetaCore™ is more feasible for pathway analysis using a relatively low number of cases, and was therefore selected to analyze the LCM samples in this study. The network processes involving genes for which the differential expression was statistically significant ($p < 0.05$) in genotype 1 patients are shown in Fig. 4. Before treatment, many of the immune mediated pathways, such as IFN-α, cell adhesion, IFN-γ, and TCR, were up-regulated in whole liver specimens from genotype 1-nonRsp compared with Rsp. Similar

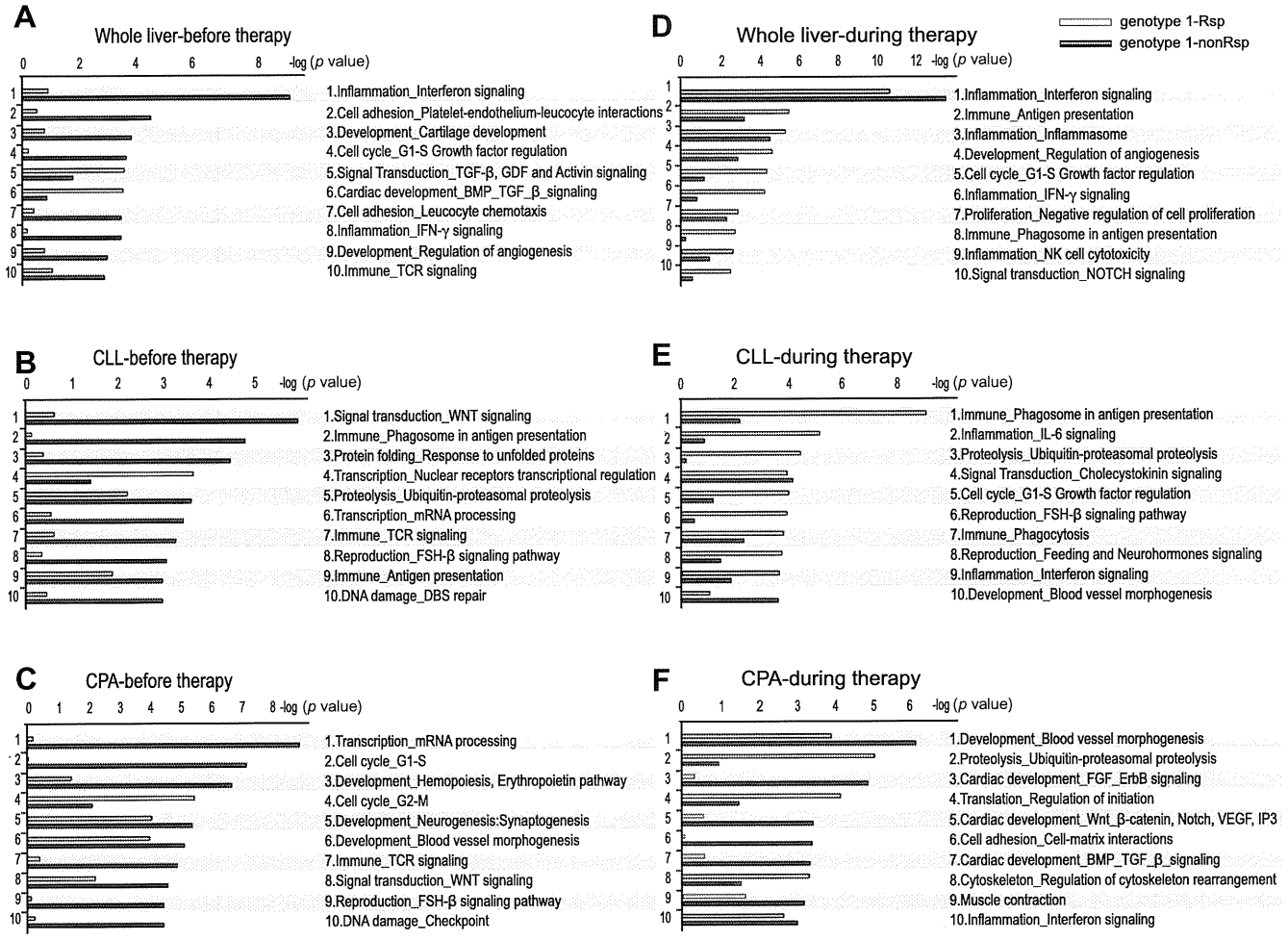

Fig. 4. Functional ontology enrichment analysis of differentially expressed genes ($p < 0.05$) using MetaCore™. GeneGo network process of differentially expressed genes between genotype 1-Rsp (white bar) and genotype 1-nonRsp (blue bar) are listed in order of decreasing statistical significance.

immune-mediated pathways were up-regulated in CLL of genotype 1-nonRsp. In CPA, many of the pathways associated with cell proliferation and DNA damage were up-regulated, reflecting the active inflammatory process in the lymphocytes of genotype 1-nonRsp (Fig. 4A–C). During treatment, many of the immune reactive pathways, such as IFN, NK cell, and antigen presenting, were induced in the whole liver and CLL specimens from genotype 1-Rsp but not in nonRsp (Fig. 4D and E). In contrast, the expression of IFN-inhibitory genes was significantly induced in CLL from nonRsp during treatment (Table 3 and Fig. 4). Interestingly, in CPA, the IFN pathway was induced in genotype 1-Rsp and nonRsp to the same degree; however, signaling pathways related to angiogenesis and fibrogenesis, such as FGF, Wnt, TGF-beta, Nocth, and VEGF signaling, were induced more in CPA from genotype 1-nonRsp than from Rsp (Figs. 3 and 4F). Thus, differential expression of signaling pathways could be observed in CLL and CPA obtained from genotype 1-Rsp and nonRsp.

Discussion

IFN and Rib combination therapy has become a commonly used modality for treating patients with CH-C, although the precise mechanism of treatment resistance is unclear. With the development of methods to quantitatively assess viral kinetics during treatment, studies were able to demonstrate that patients who cleared HCV in the early period showed favorable outcomes, whereas patients who needed a longer time to clear HCV experienced poor outcomes [4,7,17]. Thus, early clearance of virus after initiation of treatment is one of the important determinants for the complete eradication of HCV.

In this study, we analyzed gene expression from liver biopsy samples obtained before and at 1 week after initiation of treatment to investigate the precise mechanisms involved in treatment and treatment resistance. Although global gene expression profiles in the liver and PBMC during IFN treatment in a chimpanzee have been reported [12,13], the relationship between the expression profiles and clinical outcome could not be evaluated.

During the preparation of this study, two reports using a similar approach have been published [6,20]. For example, Feld et al. [6] analyzed gene expression in the livers of CH-C patients on treatment. The authors, however, compared gene expression among different patients at initiation ($n = 19$; 5 rapid responders, 10 slow responders, 4 naive) and during treatment ($n = 11$; 6 rapid responders, 5 slow responders). Because patients were not serially biopsied before and during the treatment, true treatment-related gene induction could not be evaluated. Moreover, half of the on-treatment group was administered Rib alone for three days prior to liver biopsy. In the other report, Sarasin-Filipowicz et al. [20] extensively analyzed serial liver biopsy specimens under the treatment; however, the number of the patients enrolled in their study was relatively low and heterogeneous with respect to the infected genotypes. Our study has extended their findings and provides further insights into the mechanism of IFN resistance by analyzing gene expression in CLL and CPA separately for the first time. The analysis of genotype 2 HCV also enabled us to understand the importance of the differing sensitivities to IFN between strains.

By comparing gene expression in serial liver biopsy specimens obtained at initiation and during treatment, IFN- and Rib-stimulated genes (IRSGs) in the livers of patients with CH-C could be identified (Supplementary Table 1). Our study clearly demonstrated that IRSG induction correlated with the elimination of HCV in patients with genotype 1 in accordance with previous results [6,20]. The patients who did not show a response to treatment had poor induction of IRSGs (Fig. 1A). In contrast, IRSG expression before treatment showed an opposite pattern of expression. IRSGs were induced in genotype 1-nonRsp rather than in genotype 1-Rsp. This finding was first described by Chen et al. [3] and confirmed by others [1,6,20]. Asselah et al. [1] extensively analyzed 58 curated ISGs published previously by RTD-PCR and found that three genes (IFI27, CXCL9 and IFI-6–16) were predictive of treatment outcome. However, only 12 of their 58 curated genes were also included in the 100 most up-regulated genes we observed during treatment (Supplementary Table 1). Therefore, more valuable genes for the prediction of treatment outcome might exist and our gene list could be useful for further selection of predictors of treatment outcome.

We showed that different levels of IRSG induction before treatment was associated with up-regulation of different signaling pathways, such as apoptosis and inflammatory pathways, in genotype 1-nonRsp, although histological assessment of activities and stages could not differentiate the two groups of patients. During treatment, these pathways, including the innate immune response for IFN production, were significantly induced in genotype 1-Rsp but not in genotype 1-nonRsp. The results suggest that previous up-regulation of IRSGs might be linked to impaired induction of IRSGs and contribute to poor treatment response in patients with genotype 1. Interestingly, an impaired IRSG induction was mainly noticeable in CLL, but not in CPA, and the results were confirmed by RTD-PCR (data not shown). These results suggest that IRSG induction in HCV-infected hepatocytes could play an essential role in the eradication of the genotype 1 virus in CH-C patients.

However, these scenarios did not apply in patients with genotype 2 HCV in this study. Despite the presence of active inflammation before treatment and unsatisfactory IRSG induction during treatment, these patients showed rapid responses to treatment and favorable treatment outcomes. It could be speculated that genotype 2 HCV is far more sensitive to IFN than genotype 1 HCV, and small IRSG induction might be enough to eradicate the virus. Further studies are needed to confirm these results.

We precisely analyzed the expression profiles in CLL and CPA which were obtained using the LCM method. Although IRSGs and other immune regulatory genes were similarly induced in the CPA of genotype 1-Rsp and nonRsp, more of the angiogenic- and fibrogenic-related genes were induced in CPA of genotype 1-nonRsp (Fig. 4C and F). Therefore, growth factors released from CPA might be involved in poor IRSG induction in CLL of genotype 1-nonRsp.

In summary, by comparing the hepatic gene expression in CH-C patients with different treatment outcomes, we identified a gene expression signature characteristic of IFN resistance. Our study is very important for two reasons: first, it will help in the development of new therapeutic strategies, and second, we have identified many of the genes found to be up-regulated between genotype 1-Rsp and nonRsp, which encode molecules secreted

in serum (cytokines). Therefore, the study represents a logical functional approach for the development of serum markers as predictors of response to treatment [2]. The precise mechanisms underlying these findings should be clarified further in future studies.

Conflict of interest

The authors who have taken part in this study do not have a relationship with the manufactureres of the drugs involved either in the past or present and did not recieve fundig from the manufactureres to carry out their research. The authors received support from the Japanese Society of Gastroenterology and Ministry of Helath, Labour and Welfare.

Supplementary data

Supplementary data associated with this article can be found, in the online version, at doi:10.1016/j.jhep.2010.04.036.

References

[1] Asselah T, Bieche I, Narguet S, Sabbagh A, Laurendeau I, Ripault MP, et al. Liver gene expression signature to predict response to pegylated interferon plus ribavirin combination therapy in patients with chronic hepatitis C. Gut 2008;57:516–524.
[2] Asselah T, Bieche I, Sabbagh A, Bedossa P, Moreau R, Valla D, et al. Gene expression and hepatitis C virus infection. Gut 2009;58:846–858.
[3] Chen L, Borozan I, Feld J, Sun J, Tannis LL, Coltescu C, et al. Hepatic gene expression discriminates responders and nonresponders in treatment of chronic hepatitis C viral infection. Gastroenterology 2005;128:1437–1444.
[4] Davis GL, Wong JB, McHutchison JG, Manns MP, Harvey J, Albrecht J. Early virologic response to treatment with peginterferon alfa-2b plus ribavirin in patients with chronic hepatitis C. Hepatology 2003;38:645–652.
[5] Desmet VJ, Gerber M, Hoofnagle JH, Manns M, Scheuer PJ. Classification of chronic hepatitis: diagnosis, grading and staging. Hepatology 1994;19: 1513–1520.
[6] Feld JJ, Nanda S, Huang Y, Chen W, Cam M, Pusek SN, et al. Hepatic gene expression during treatment with peginterferon and ribavirin: identifying molecular pathways for treatment response. Hepatology 2007;46: 1548–1563.
[7] Ferenci P, Fried MW, Shiffman ML, Smith CI, Marinos G, Goncales Jr FL, et al. Predicting sustained virological responses in chronic hepatitis C patients treated with peginterferon alfa-2a (40 KDa)/ribavirin. J Hepatol 2005;43: 425–433.
[8] Fried MW, Shiffman ML, Reddy KR, Smith C, Marinos G, Goncales Jr FL, et al. Peginterferon alfa-2a plus ribavirin for chronic hepatitis C virus infection. N Engl J Med 2002;347:975–982.
[9] Germer JJ, Harmsen WS, Mandrekar JN, Mitchell PS, Yao JD. Evaluation of the COBAS TaqMan HCV test with automated sample processing using the MagNA pure LC instrument. J Clin Microbiol 2005;43:293–298.
[10] He XS, Ji X, Hale MB, Cheung R, Ahmed A, Guo Y, et al. Global transcriptional response to interferon is a determinant of HCV treatment outcome and is modified by race. Hepatology 2006;44:352–359.
[11] Honda M, Yamashita T, Ueda T, Takatori H, Nishino R, Kaneko S. Different signaling pathways in the livers of patients with chronic hepatitis B or chronic hepatitis C. Hepatology 2006;44:1122–1138.
[12] Huang Y, Feld JJ, Sapp RK, Nanda S, Lin JH, Blatt LM, et al. Defective hepatic response to interferon and activation of suppressor of cytokine signaling 3 in chronic hepatitis C. Gastroenterology 2007;132:733–744.
[13] Lanford RE, Guerra B, Bigger CB, Lee H, Chavez D, Brasky KM. Lack of response to exogenous interferon-alpha in the liver of chimpanzees chronically infected with hepatitis C virus. Hepatology 2007;46: 999–1008.
[14] Layden TJ, Layden JE, Reddy KR, Levy-Drummer RS, Poulakos J, Neumann AU. Induction therapy with consensus interferon (CIFN) does not improve sustained virologic response in chronic hepatitis C. J Viral Hepat 2002;9:334–339.
[15] Neumann AU, Lam NP, Dahari H, Gretch DR, Wiley TE, Layden TJ, et al. Hepatitis C viral dynamics in vivo and the antiviral efficacy of interferon-alpha therapy. Science 1998;282 (5386):103–107.
[16] Okamoto H, Tokita H, Sakamoto M, Horikita M, Kojima M, Iizuka H, et al. Characterization of the genomic sequence of type V (or 3a) hepatitis C virus isolates and PCR primers for specific detection. J Gen Virol 1993;74: 2385–2390.
[17] Payan C, Pivert A, Morand P, Fafi-Kremer S, Carrat F, Pol S, et al. Rapid and early virological response to chronic hepatitis C treatment with IFN alpha2b or PEG-IFN alpha2b plus ribavirin in HIV/HCV co-infected patients. Gut 2007;56:1111–1116.
[18] Rosen HR, Ribeiro RR, Weinberger L, Wolf S, Chung M, Gretch DR, et al. Early hepatitis C viral kinetics correlate with long-term outcome in patients receiving high dose induction followed by combination interferon and ribavirin therapy. J Hepatol 2002;37:124–130.
[19] Sakai Y, Honda M, Fujinaga H, Tatsumi I, Mizukoshi E, Nakamoto Y, et al. Common transcriptional signature of tumor-infiltrating mononuclear inflammatory cells and peripheral blood mononuclear cells in hepatocellular carcinoma patients. Cancer Res 2008;68:10267–10279.
[20] Sarasin-Filipowicz M, Oakeley EJ, Duong FH, Christen V, Terracciano L, Filipowicz W, et al. Interferon signaling and treatment outcome in chronic hepatitis C. Proc Natl Acad Sci USA 2008;105:7034–7039.
[21] Younossi ZM, Baranova A, Afendy A, Collantes R, Stepanova M, Manyam G, et al. Early gene expression profiles of patients with chronic hepatitis C treated with pegylated interferon-alfa and ribavirin. Hepatology 2009;49:763–774.

La Protein Required for Internal Ribosome Entry Site–Directed Translation Is a Potential Therapeutic Target for Hepatitis C Virus Replication

Takayoshi Shirasaki,[1,2] Masao Honda,[1,2] Hideki Mizuno,[1] Tetsuro Shimakami,[1] Hikari Okada,[1] Yoshio Sakai,[1] Seishi Murakami,[3] Takaji Wakita,[4] and Shuichi Kaneko[1]

[1]Department of Gastroenterology, [2]Department of Advanced Medical Technology, Division of Health Medicine, Graduate School of Medicine, [3]Division of Molecular Cell Signaling, Cancer Research Institute, Kanazawa University, Kanazawa, and [4]Department of Virology II, National Institute of Infectious Diseases, Tokyo, Japan

Background. Translation of the hepatitis C virus (HCV) is mediated by an internal ribosome entry site (IRES). Here, we analyzed the functional relevance of La protein for replication of HCV using an infectious HCV clone, JFH-1.

Methods. A single-nucleotide mutation from A to U was introduced at the 338th nucleotide in the stem-loop domain IV structure of HCV IRES, which stabilized stem-loop IV and abolished translation and replication of JFH-1 almost completely.

Results. During JFH-1 replication, translation initiation factors required for HCV IRES activity, including La protein, polypyrimidine tract binding protein (PTB), PSMA7, and PCBP2, were significantly induced in Huh-7.5 cells. Interestingly, JFH-1 infection increased telomerase activity and induced the expression of human telomerase RNA (hTR) in Huh-7.5 cells. In 37 tissue specimens from patients with chronic hepatitis C, La protein significantly correlated with the representative essential telomerase components hTR, p23, and HSP90 ($P < .001$). Recombinant adenovirus that expressed short-hairpin RNA against La protein successfully suppressed the levels of La protein and core protein of JFH-1 to 30% of that in the control cells.

Conclusions. HCV infection might be strongly related to telomerase activity in the liver through La protein induction. Inhibition of La protein substantially repressed JFH-1 replication; therefore, La protein is a potential therapeutic target for HCV.

Hepatitis C virus (HCV) is a positive-strand, enveloped RNA virus that belongs to the genus *Hepacivirus* in the family *Flaviviridae*. A human liver infected with HCV develops chronic hepatitis, cirrhosis, and in some instances, hepatocellular carcinoma [1]. Although a combination of ribavirin and interferon has become a routine means of treating infected patients, the results are often unsatisfactory, especially in patients with a high viral load [2]. Identification of host factors that regulate HCV replication in infected patients could be helpful in the development of a novel antiviral treatment strategy. It has been reported that various host factors are associated with HCV infection; however, only a few proteins have been functionally shown with an infectious HCV clone to regulate HCV replication [3].

The translation of HCV is initiated by a highly structured RNA segment, the internal ribosome entry site (IRES), which occupies most of the 5′ nontranslated RNA [4]. Many canonical and noncanonical translation initiation factors, such as La protein [5], polypyrimidine tract binding protein (PTB) [6], and eukaryotic initiation factor 3 (eIF3), interact with HCV IRES and might regulate HCV translation. Previously, we reported that HCV IRES activity is highly dependent on these initiation factors, and it correlated with the expression of La protein [7, 8]. However, the functional relevance of these translation initiation factors on HCV

Received 17 September 2009; accepted 6 January 2010; electronically published 24 May 2010.

Potential conflicts of interest: none reported.

Financial support: This study is partially supported by the Grants-in-Aid for Scientific Research by Japan Society for the Promotion of Science (project 17591036).

Reprints or correspondence: Dr Masao Honda, Department of Gastroenterology, Graduate School of Medicine, Kanazawa University, Takara-Machi 13-1, Kanazawa 920-8641, Japan (mhonda@m-kanazawa.jp).

The Journal of Infectious Diseases 2010;202(1):75–85

0022-1899/2010/20201-0009$15.00
DOI: 10.1086/653081

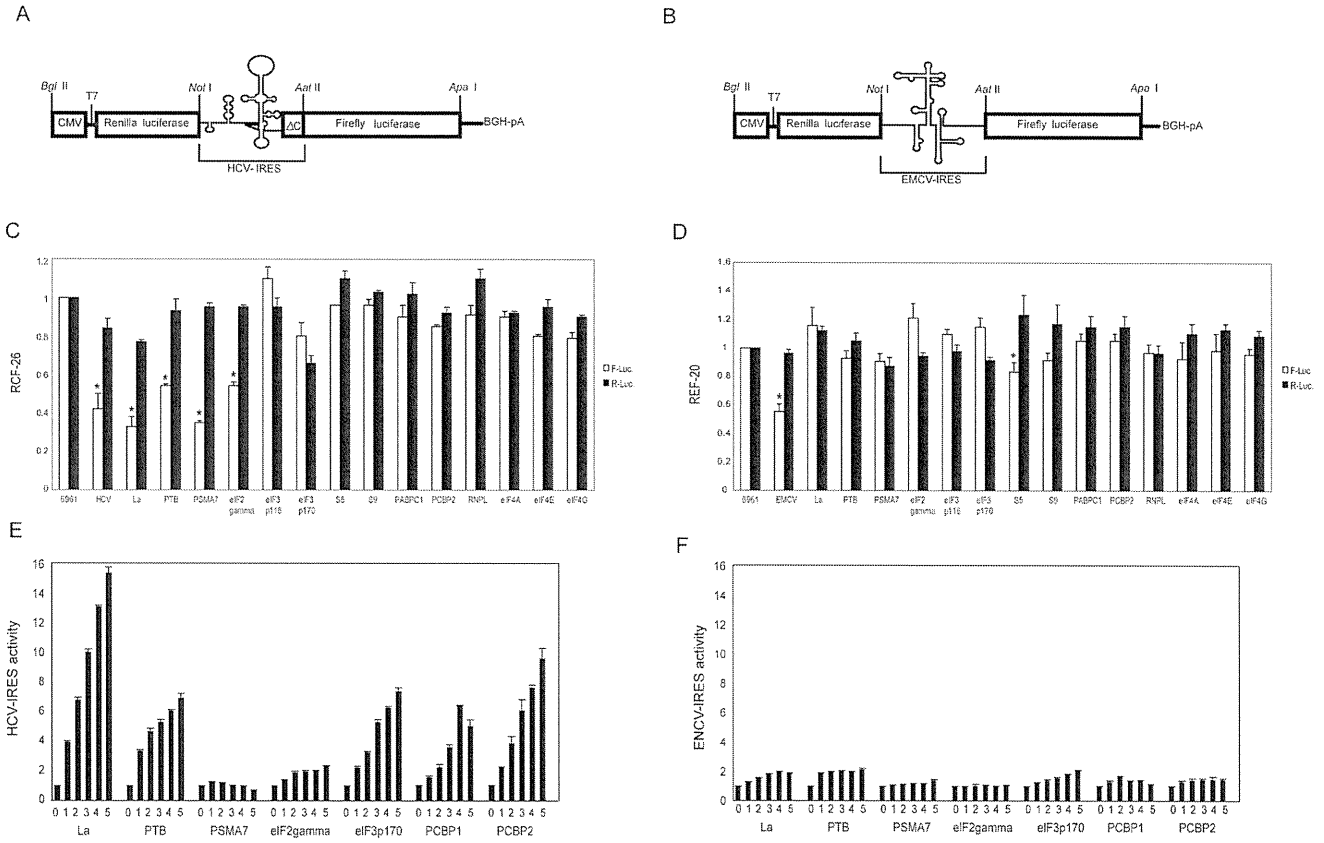

Figure 1. Organization of the transcriptional unit of plasmids pRL-HL (*A*) and pRL-EL (*B*). *C* and *D*, Suppression of 14 canonical and noncanonical initiation factors by specific antisense oligonucleotides. Changes in *Renilla* luciferase (RL) and firefly luciferase (FL) (hepatitis C virus–internal ribosome entry site [HCV-IRES]–directed translation) activities in RCF-26 (*C*). Changes in RL and FL (encephalomyocarditis virus [ENCV]–IRES–directed translation) activities in REF-20 (*D*). **P* < .05. *E* and *F*, In vitro translation of pRL-HL and pRL-EL in rabbit reticulocyte lysate. The plasmids pRL-HL or pRL-EL (0.05 μg) and increasing amounts of expression vectors (0–0.125 μg) of La protein, polypyrimidine tract binding protein (PTB), eIF3p 170, eIF2γ, PSMA7, PCBP1, and PCBP2 were co-translated in rabbit reticulocyte lysate. The fold increases in relative HCV IRES activity (*E*) and ENCV-IRES activity (*F*) are shown. **P* < .05. *Lane 0*, 0 μg; *lane 1*, 0.025 μg; *lane 2*, 0.05 μg; *lane 3*, 0.075 μg; *lane 4*, 0.1 μg; *lane 5*, 0.125 μg. **P* < .05.

replication had not been fully evaluated. In this study, we found that the expression of La protein is induced by HCV infection, and this induced La protein–activated telomerase activity in a human hepatoma cell line. The results indicate La protein is a potential therapeutic target for HCV infection.

EXPERIMENTAL PROCEDURES

Expression vector plasmids. The FLAG tag fusion La protein expression vector (pCMV-La-FLAG) was created by polymerase chain reaction (PCR), using the La protein expression vector (pCMV-La) as the template [8]. The forward primer 5′-AAT GAA ATC AGA AGA AA-3′ contains an *Xba* I site, and the reverse primer 5′-TGA TCT AGA TTA CTT ATC GTC GTC ATC CTT GTA ATC CTG GTC TCC AGC ACC ATT TTC TGT TTT CTG TTG -3′ contains *Xba* I and FLAG sites.

Cell lines. Human hepatocellular carcinoma 7 (Huh-7) cells and Huh-7.5 cells (provided by Professor C. M. Rice, Rockefeller University) were maintained in Dulbecco modified Eagle medium (DMEM; Gibco BRL), which contained 10% fetal bovine serum and 1% penicillin/streptomycin. The RCF-26 was a stably transformed cell line from Huh-7 cells that constitutively expressed dicistronic RNA transcripts containing sequences encoding 2 reporter proteins—*Renilla* luciferase and firefly luciferase—separated by a functional HCV IRES of genotype 1b (Figure 1*A*) [7]. The REF-20 was a stably transformed cell line from Huh-7 cells that constitutively expressed dicistronic RNA transcripts in which HCV IRES was replaced with encephalomyocarditis virus (EMCV) IRES (Figure 1*B*).

Antisense oligodeoxynucleotide. The antisense phosphorothioate oligodeoxynucleotides (oligos) designed for HCV IRES, La protein, PTB, eIF3, eIF2γ, S9, poly(A)-binding protein cytoplasmic 1 (PABPC1), PCBP2, RNPL, and control randomized oligo 6961 were described elsewhere [8]. Antisense oligos for PSMA7, S5, eIF4A, eIF4E, eIF4G, and EMCV IRES were synthesized. The nucleotide sequences of the antisense oligos were 5′-CTC ATG CCG GCG GGC GGC CG-3′ for PSMA7,

5′-GTC ATC CTG AGA ACA CAG CC-3′ for S5, 5′-GAC ATG ATC CTT AGA AAC TA-3′ for eIF4A, 5′-GCC ATC TTA GAT CGA TCT GA-3′ for eIF4E, 5′- GAC ATG ATC TCC TCT GTG AT-3′ for eIF4G, and 5′-TCC ATA TTA TCA TCG TGT TT-3′ for EMCV IRES. The antisense oligos (1.0 μmol/L) were transfected into RCF-26 (Figure 1*C*) or REF-20 (Figure 1*D*). After 24 h of transfection, *Renilla* luciferase (cap-dependent translation) and firefly luciferase (HCV or EMCV-directed translation) activities were measured with the Dual-Luciferase Reporter Assay System (Promega).

In vitro translation of pRL-HL and pRL-EL in rabbit reticulocyte lysate. In vitro translation of pRL-HL and pRL-EL was carried out in transcription and translation–coupled rabbit reticulocyte lysate systems (Promega). In 25 μL of the transcription and translation reaction mixture, 0.05 μg of pRL-HL or pRL-EL was cotranslated with an increasing amount of plasmid DNA (up to 0.125 μg) of La, PTB, PSMA7, eIF2-γ, eIF3p170, PCBP1, and PCBP2, which were cloned using the T7 promoter. A 3-μL aliquot was then used to measure *Renilla* luciferase and firefly luciferase activities using the Dual-Luciferase Reporter Assay System (Promega).

Site-directed mutagenesis. The plasmid pJFH-1 was used as the template for introduction of the site-directed mutation at nucleotide 338 in the 5′ nontranslated RNA. The site-directed mutagenesis reaction was performed using the Pfu Turbo DNA polymerase PCR system (Stratagene), according to the manufacturer's instructions.

Transfection of JFH-1 and JFH-1 338U into Huh-7.5 cells. Ten micrograms of synthetic RNA transcribed from pJFH-1 or pJFH-1 338U was used for electroporation. Cells were then pulsed at 260 V and 950 μF using the Gene Pulser II apparatus (Bio-Rad Laboratories).

Infection of Huh-7.5 cells with JFH-1. Seventy-two hours after transfection, the culture medium was collected, cleared by low-speed centrifugation at 2000 revolutions per minute at 760g for 10 min, and passed through a Millipore filter (pore size, 0.45 μm; Millipore Corporation). Part of the filtered culture medium was diluted 50-fold or 10-fold with DMEM containing 10% fetal bovine serum and 1% penicillin-streptomycin. Diluted culture medium (1 mL) was used for injection of cells into a well of a 6-well plate or a well containing cover slips and incubated for 4 h. At 3 days after infection, inoculated cells grown on cover slips were fixed and stained using anti-core antibody, as described below. The amounts of HCV RNA, La-RNA, and human telomerase RNA (hTR)-RNA in inoculated cells were determined by quantitative real-time detection (RTD)-PCR.

Western blot analysis and immunofluorescence staining. The expression levels of La protein and PTB in cells were evaluated by Western blotting using mouse anti-La antibody (SW5) and rabbit anti-PTB antibody, as described elsewhere [9]. The expression of HCV core protein, PSMA7, eIF2γ, PCBP2, and FLAG-tagged La protein was evaluated with mouse anti-core antibody (Affinity BioReagents), mouse anti-PSMA7 antibody (Antibodies Direct), rabbit anti-eIF2γ antibody (Abcam), mouse anti-huRNP E2 (23-G) antibody (Santa Cruz Biotechnology), and mouse anti-FLAG antibody (Sigma), respectively. For immunofluorescence staining, anti–core monoclonal antibodies and Alexa Fluor 488 goat anti–mouse immunoglobulin G antibody (Invitrogen) were used.

Quantitative RTD-PCR. The primer pairs and probes for La protein, PTB, eIF3 p170, GAPDH, and HCV were obtained as described elsewhere [8]. The primer pairs and probes for PSMA7, eIF2γ, PCBP2, hTR, p23, Hps90, and β-actin were obtained from the TaqMan assay reagents library. One microgram of isolated RNA was reverse-transcribed to complementary DNA using SuperScript II RT (Invitrogen) according to the manufacturer's instructions, and the resulting complementary DNA was amplified with appropriate TaqMan assay reagents [10].

Telomerase activity assay. The plasmids pCMV-La-FLAG and pCR3.1 were transfected into Huh-7 cells using Fugene 6 transfection reagent (Roche Applied Science). Forty-eight hours after transfection, the amounts of hTR-RNA in the transfected cells were determined by RTD-PCR. The expression of the FLAG-tag fusion La protein was evaluated by Western blot analysis. Telomerase activity was measured with a PCR-based telomerase repeat amplification protocol (TRAP) assay, performed with the TRAPEZE kit (Invitrogen) according to the manufacturer's instructions. Each reaction product was amplified in the presence of a 36-base pair internal telomerase assay standard. The PCR products were fractionated by electrophoresis on a 10% polyacrylamide gel and then visualized by staining with SYBR Green (Molecular Probes).

Construction of recombinant adenovirus expressing short-hairpin RNA for La protein. The short-hairpin RNA expression plasmid (pSh-La), which expresses short-hairpin RNA for La protein (seq: 5′-CCG GCC AAG GCA GAA CTC ATG GAA ACT CGA GTT TCC ATG AGT TCT GCC TTG GTT TG-3′), was purchased from Sigma. The pSh-La was digested with the enzymes *Hin*d III and *Bam*HI, and the excised fragment, including the short-hairpin RNA, was transferred to the adenoviral expression plasmid. The adenoviral expression plasmid and bovine growth hormone plasmid were cotransfected into 293A cells using the CellPhect Transfection kit (GE Healthcare) to produce crude adenoviral stocks. These stocks were purified using the Adeno-X Virus Purification kit (Clontech Laboratories) and stored at −80°C. The titers of the adenoviral stocks were adjusted to 4.0×10^9 PFU/mL.

Twelve hours after JFH-1 RNA transfection, the cells were washed 3 times with phosphate-buffered saline, and then Ad-shLa or Ad-Null was added at a multiplicity of infection of 10.

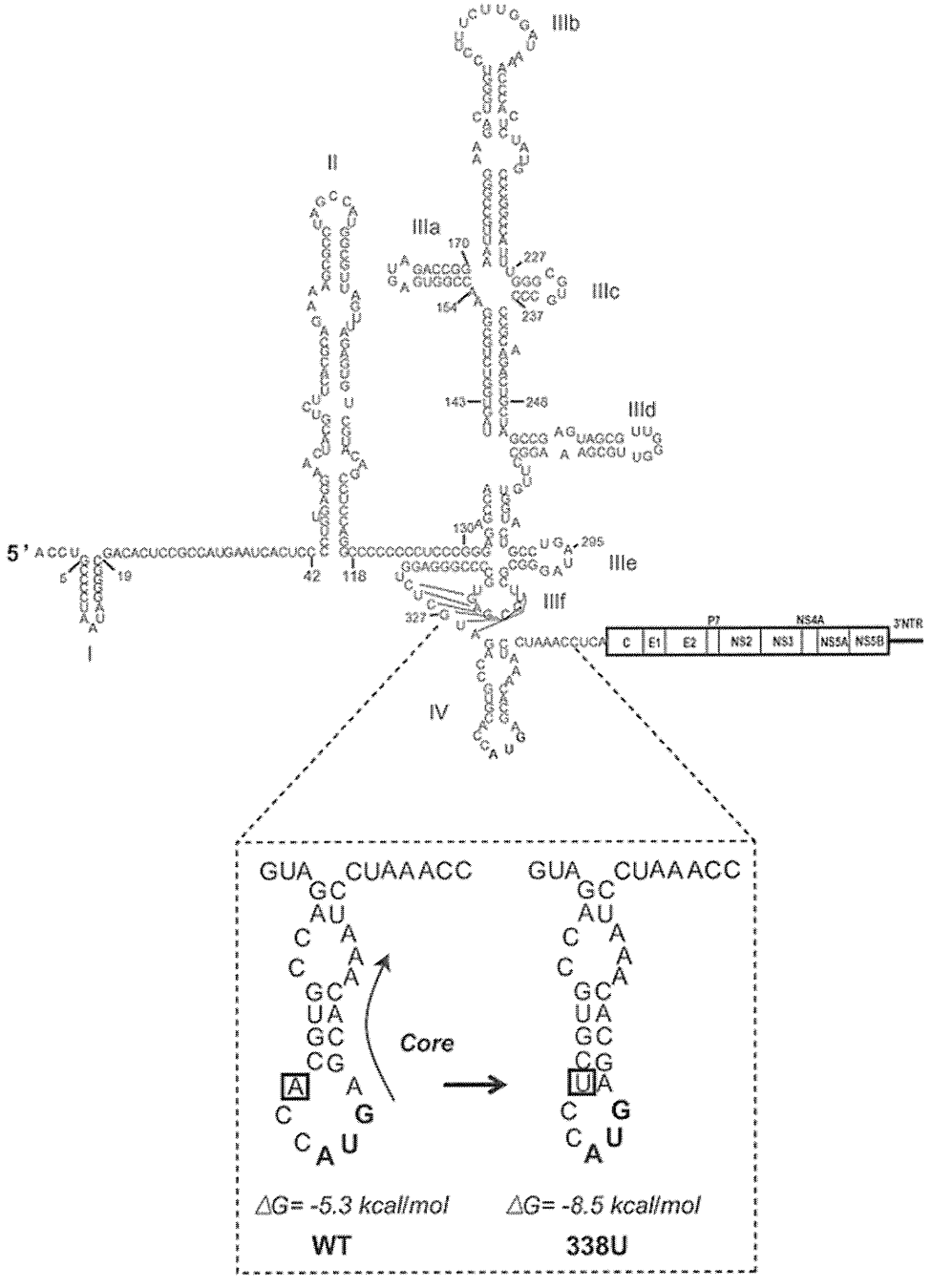

Figure 2. Organization of the full-length JFH-1 and the mutation at nucleotide 338 of stem loop IV.

One hour after injection, the cells were washed 3 times with phosphate-buffered saline, and complete culture medium was added.

Statistical analysis. Results were expressed as mean values ± standard deviation. Significance was tested by 1-way analysis of variance with Bonferroni methods, and differences were considered statistically significant at $P < .05$.

RESULTS

Dependence of HCV IRES activity on translation initiation factors. To confirm that HCV IRES activity was highly dependent on translation initiation factors, antisense oligonucleotides designed for 14 translation initiation factors were transfected into RCF-26 and REF-20 cells, and HCV or EMCV IRES

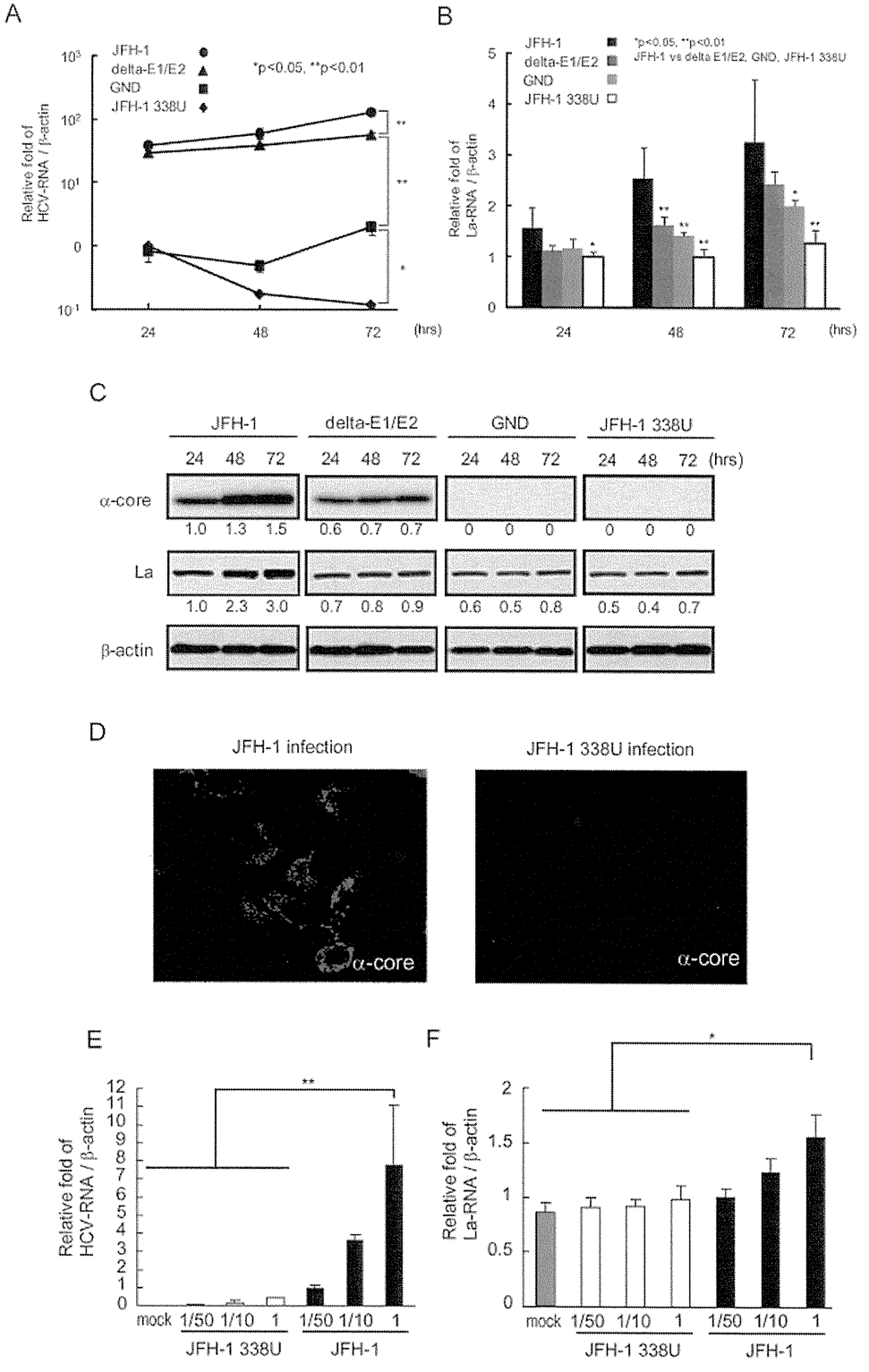

Figure 3. *A*, Hepatitis C virus (HCV) RNA replication determined by real-time detection–polymerase chain reaction (RTD-PCR) in JFH-1, JFH-1/delta E1-E2, JFH-1/GND, and JFH-1 338U transfected cells. $^{*}P < .05$. $^{**}P < .01$. *B*, La RNA expression determined by RTD-PCR in JFH-1, JFH-1/delta E1-E2, JFH-1/GND, and JFH-1 338U transfected cells. $^{*}P < .05$. $^{**}P < .01$. *C*, Western blots for detection of HCV core protein and La protein in JFH-1, JFH-1/delta E1-E2, JFH-1/GND and JFH-1 338U transfected cells. *D*, Immunofluorescence staining of core protein in Huh-7.5 cells infected with JFH-1 or JFH-1 338U. *E* and *F*, HCV RNA and La RNA determined by RTD-PCR in Huh-7.5 cells infected with serial dilution of JFH-1 or JFH-1 338U. $^{*}P < .05$, $^{**}P < .01$.

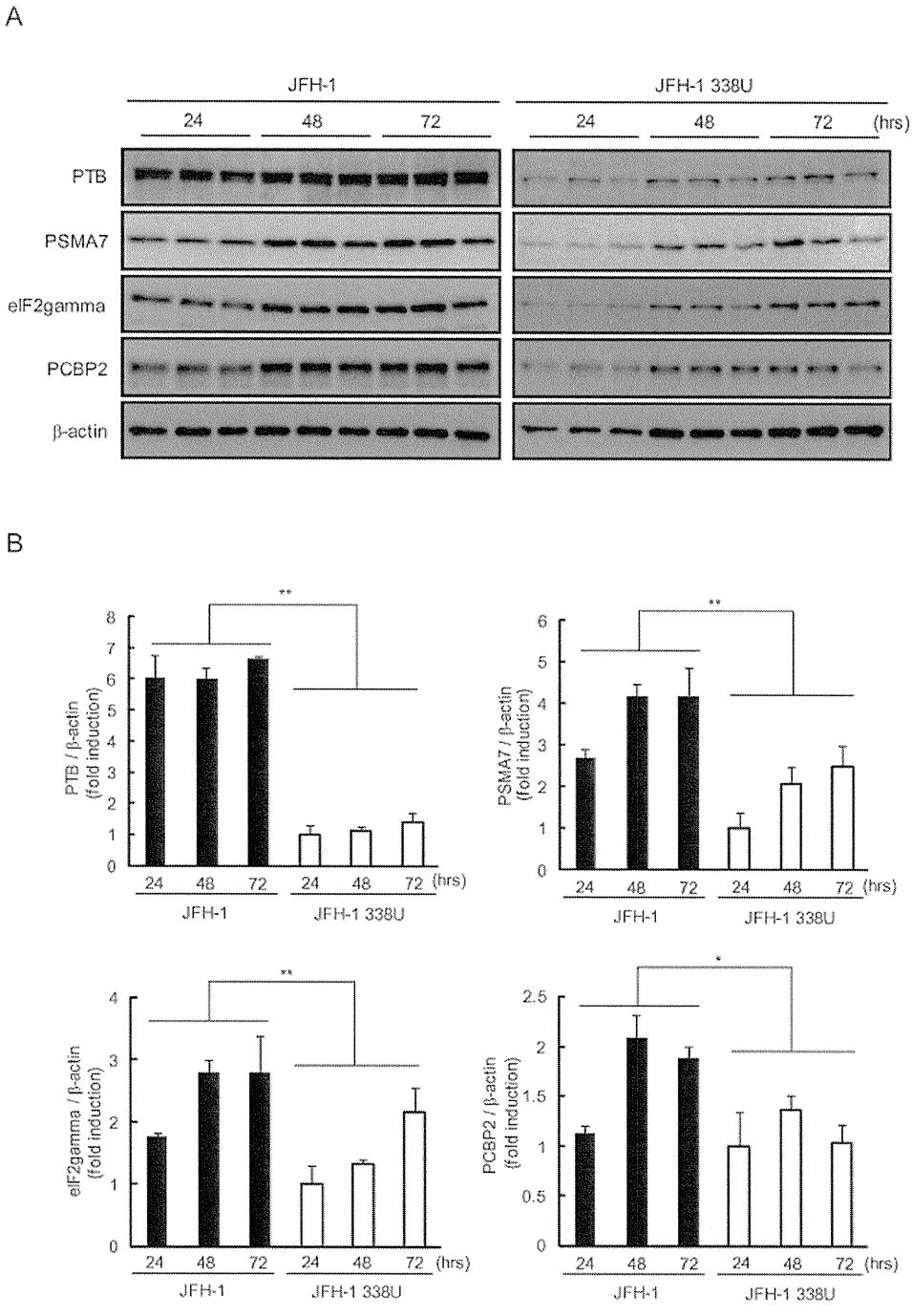

Figure 4. *A*, Protein expression of PTB, PSMA7, eIF2γ, and PCBP2 determined with Western blotting in Huh-7.5 cells after transfection with JFH-1 RNA and JFH-1 338U RNA. *B*, Quantitative densitometric analysis of protein expression. $^{*}P < .05$, $^{**}P < .01$.

activity was evaluated. The activities of *Renilla* luciferase and firefly luciferase expressed in these cells reflect cap-dependent and HCV or EMCV IRES directed translation, respectively (Figure 1*B* and 1*C*). The suppression of La protein, PTB, PSMA7, and eIF2γ by the antisense oligonucleotides in RCF-26 significantly repressed firefly luciferase activities, whereas *Renilla* luciferase activities were mostly maintained (Figure 1*C*). In contrast, these translation initiation factors did not affect EMCV IRES activity in REF-20 cells (Figure 1*D*).

These findings were also evaluated in rabbit reticulocyte lysates (RRL). With increasing amounts of expression vectors or La protein, PTB and eIF3 p170, the HCV IRES activity increased significantly (7-fold to16-fold) (Figure 1*E*). Although the depletion of PCBP2 did not affect HCV IRES activity in the RCF-

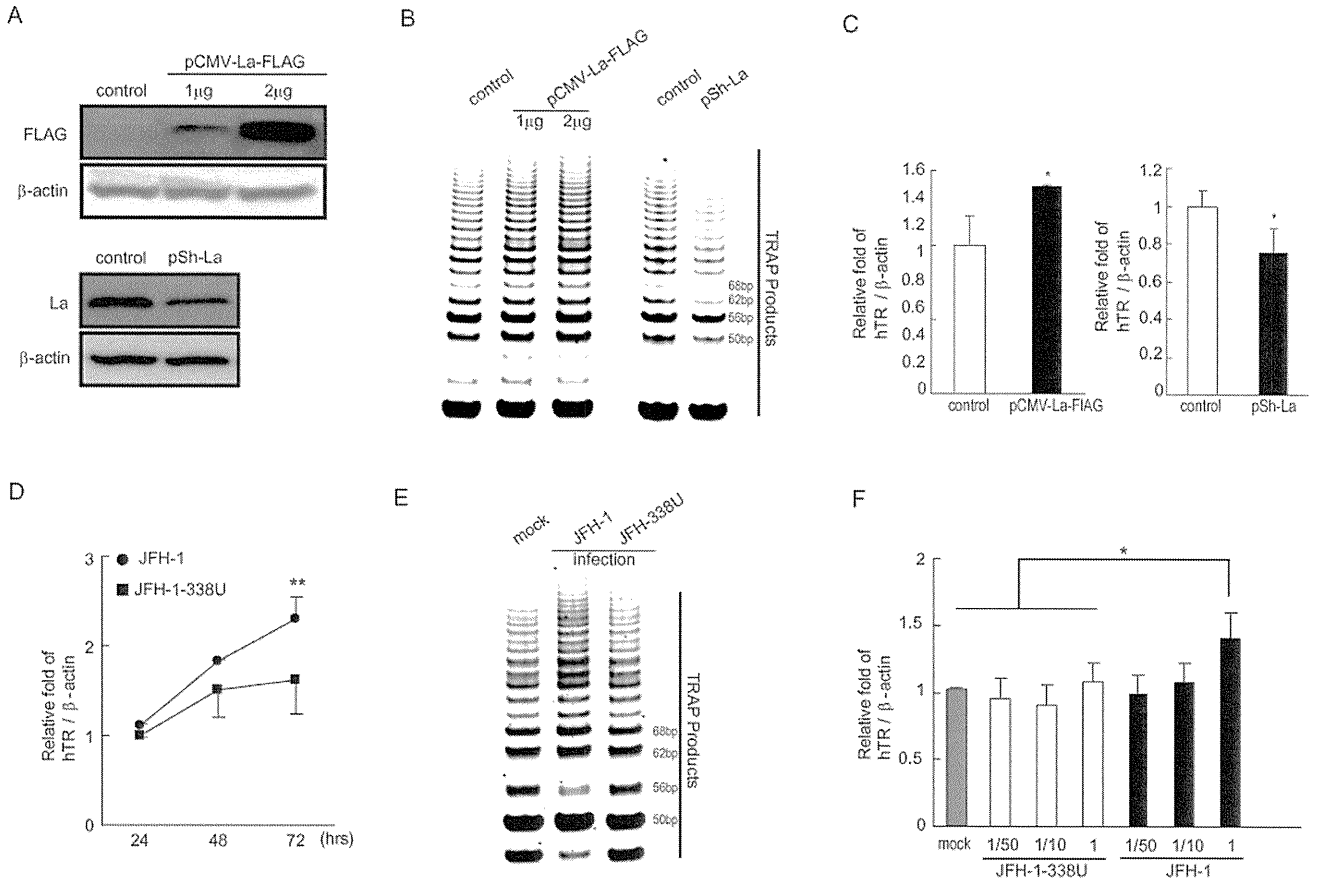

Figure 5. *A*, Western blot analysis of pCMV-La-FLAG or pSh-La transfected Huh-7 cells. *B*, The telomerase repeat amplification protocol (TRAP) assay in pCMV-La-FLAG or pSh-La transfected Huh-7 cells. *C*, Human telomerase RNA (hTR) expression in pCMV-La-FLAG or pSh-La transfected Huh-7 cells by real-time detection–polymerase chain reaction (RTD-PCR). $^{*}P < .05$. *D*, The hTR expression in JFH-1 or JFH-1 338U RNA-transfected Huh-7.5 cells by RTD-PCR. $^{**}P < .01$. *E*, The TRAP assay in JFH-1 or JFH-1 338U infected Huh-7 cells. *F*, Effect of JFH-1 or JFH-338U infection on hTR expression in Huh-7.5 by RTD-PCR. $^{*}P < .05$.

26 cells, it stimulated HCV IRES activity up to 10-fold in the RRL (Figure 1*E*). On the other hand, EMCV IRES activity increased modestly by up to 2-fold (Figure 1*F*). These findings confirmed previous findings that HCV IRES activity is highly dependent on cellular factors.

Construction of translation incompetent full-length infectious HCV clone. JFH-1 is a genotype 2a-derived full length infectious HCV clone [11]. To evaluate the essential role played by IRES activity in HCV replication, we constructed a translation incompetent JFH-1 by introducing a single-nucleotide mutation from adenine to uracil at the position of nucleotide 338 (the third nucleotide upstream of the initiation codon of the core protein) in the 5′ nontranslated RNA (JFH-1 338U) (Figure 2). This mutation decreased the free energy (ΔG = 5.3 to −8.5 kcal/mol) and stabilized the folding structure of stem-loop domain IV that includes the initiation codon of the core protein. This mutation impairs ribosomal access to the AUG codon for translation initiation of viral proteins, as reported elsewhere [12].

Transfection of JFH-1 RNA into Huh-7.5 cells resulted in a substantial increase in viral RNA and core protein, as determined with RTD-PCR (Figure 3*A*), indirect immunofluorescence staining (data not shown), and Western blot analysis (Figure 3*C*). In contrast, translation-incompetent JFH-1 338U resulted in no evidence of viral replication or protein translation (as shown in Figure 3*A* and 3*C*). This indicated the functional importance of stem-loop IV not only for translation initiation but also for viral replication. Therefore, we used JFH-1 338U as an appropriate negative control in additional experiments.

Expression of La protein induced by JFH-1 in Huh-7.5 cells. Previously, we reported that expression of La protein was induced in the livers of patients with chronic hepatitis C, and the expression of La protein showed significant correlation with HCV RNA in tissue specimens from these patients [8]. In this study, we explored whether HCV might directly induce expression of La protein. The synthetic RNAs of JFH-1, JFH-1/delta E1-E2, JFH-1/GND [11], and JFH-1 338U were transfected into Huh-7.5 cells, and the expression of La RNA was

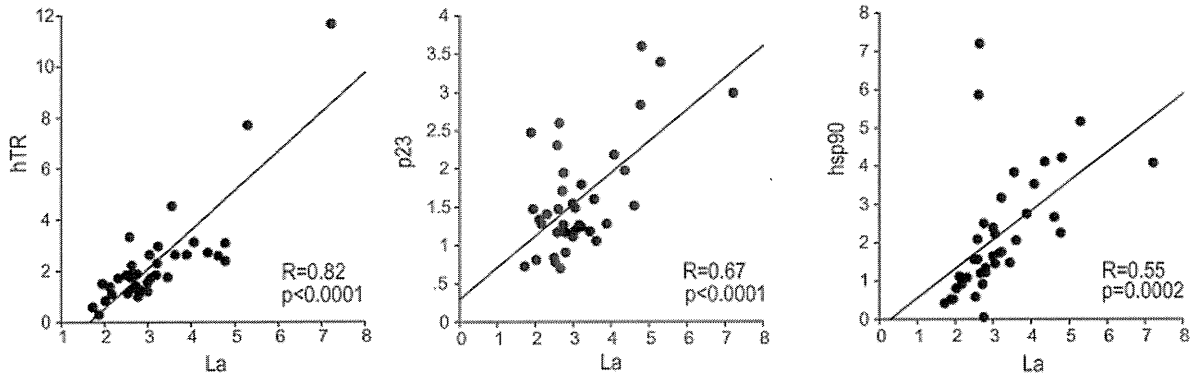

Figure 6. Correlation between expression of La protein and activity of human telomerase RNA (hTR), p23, and Hsp90 in liver biopsy specimens obtained from 37 patients with chronic hepatitis C.

evaluated after transfection by RTD-PCR and Western blot analysis. JFH-1 RNA peaked at 72 h after transfection (Figure 3*A*), as did the level of HCV core protein (Figure 3*C*). The JFH-1/delta E1-E2 RNA peak was significantly hampered compared with JFH-1 owing to the defective feature of infection. JFH-1 338U RNA and JFH-1/GND RNA was almost negligible at 72 h after transfection (Figure 3*A*) and a significant decline in JFH-1 338U RNA was noted. Under these conditions, La RNA was mostly induced in Huh-7.5 cells transfected with JFH-1, compared with JFH-1/delta E1-E2, JFH-1/GND, and JFH-1 338U (Figure 3*B*).

Similarly, expression of La protein was significantly increased after JFH-1 replication in Huh-7.5 cells, whereas only a slight increase was noticed in Huh-7.5 cells transfected with JFH-1/GND or JFH-1 338U (Figure 3*C*). The results indicated that JFH-1 replication induced La protein in Huh-7.5 cells.

To examine these findings further, the culture medium of the Huh-7.5 cells that included infectious HCV particles was collected and used to infect fresh Huh-7.5 cells at dilutions of 1:1, 1:10, and 1:50. HCV infection in the Huh-7.5 cells was confirmed by the expression of core protein (Figure 3*D*) and the presence of HCV RNA (Figure 3*E*). HCV infection was dependent on the amount of inoculated virus, as shown in Figure 3*E*. In contrast, there was no evidence of infection when using culture medium from Huh-7.5 cells transfected with JFH-1 338U RNA (Figure 3*D*, 3*E*). La RNA was significantly increased by the infection of virus derived from JFH-1 but not that derived from JFH-1 338U (Figure 3*F*). These results suggest that HCV infection itself could induce La protein in Huh-7.5 cells.

As for other initiation factors such as PTB, PSMA7, eIF2γ, and PCBP2, which were shown to be essential factors for HCV IRES activity (Figure 1), we also evaluated their gene expression according to the replication of JFH-1 (Figure 4). Western blotting of each initiation factor after JFH-1 RNA transfection showed significantly increased PTB, PSMA7, eIF2γ, and PCBP2. The increase was significantly greater in JFH-1 RNA transfected cells than in JFH-1 338U RNA transfected cells. Thus, HCV induces these initiation factors, and in turn, they served for HCV replication. Importantly, these relationships might be true in the tissue lesions of chronic hepatitis C. There were also significant correlations between the expression of these initiation factors and HCV RNA in the tissue specimens from patients with chronic hepatitis C, although the correlation between PTB, eIF3 p170, and HCV RNA was less than La protein, PSMA7, eIF2γ, PCBP2, and HCV RNA (data not shown) [8].

Activation of telomerase activity by La protein through the increase of human telomerase RNA. We next investigated the functional relevance of induced La protein in hepatocytes. Human telomerase plays an important role in cellular senescence and carcinogenesis. Human telomerase reverse transcriptase and hTR, as an RNA template, are core components of telomerase activity. In addition, other telomerase components, such as Hsp90 and p23 [13], have been reported to be essential for telomerase activity. There is a report that La protein is one of the telomerase components interacting with hTR [14]; however, the functional relevance of La protein for telomerase activity has not yet been validated.

The FLAG-tagged La protein expression vector pCMV-La-FLAG or short-hairpin RNA for La protein expression vector pSh-La was transfected into Huh-7 cells, and transduction was confirmed by Western blotting using anti-FLAG antibody or anti-La protein antibody (Figure 5*A*). Telomerase activity detected by the TRAP assay in cells overexpressing La protein was significantly higher than that found in control cells. In contrast, telomerase activity was repressed in La protein–repressed Huh-7 cells (Figure 5*B*). To reveal the mechanism underlying the up-regulation of telomerase activity by La protein, we measured the changes in the expression of human telomerase reverse transcriptase and hTR by RTD-PCR. Although no significant changes were observed in the expression of human telomerase

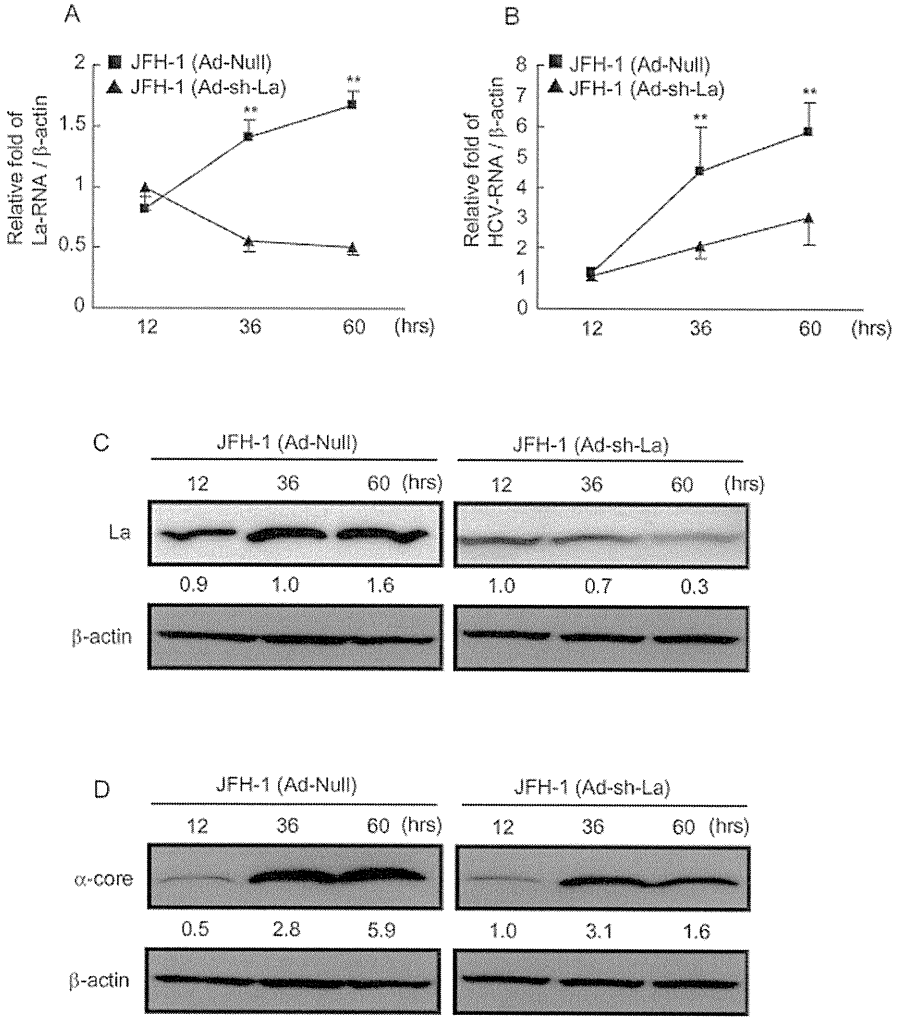

Figure 7. Suppression of La protein expression and its effect on of hepatitis C Virus (HCV) replication. *A*, Effect of Ad-shLa on La protein expression in JFH-1-transfected cells. $^{**}P < .01$. *B*, Effect of Ad-shLa on HCV replication. $^{**}P < .01$. *C*, Western blotting of La protein in JFH-1-transfected Huh-7.5 cells after infection with Ad-Null or Ad-shLa. *D*, Western blotting of HCV core protein in JFH-1-transfected Huh-7.5 cells after infection with Ad-Null or Ad-shLa.

reverse transcriptase, the expression of hTR was modestly but significantly increased by the overexpression of La protein and decreased by the repression of La protein, respectively (Figure 5*C*).

This finding was confirmed in Huh-7.5 cells transfected with JFH-1 RNA, which showed significantly higher expression of hTR than those transfected with translation-replication incompetent JFH-1 338U (Figure 5*D*). Moreover, JFH-1 infection similarly activated telomerase activity (Figure 5*E*) and induced hTR (Figure 5*F*) in Huh-7.5 cells, whereas JFH-1 338U infection did not activate telomerase activity or induce hTR. Therefore, the data strongly suggest that HCV infection could activate telomerase activity by increasing La protein and hTR.

When the relationship between La protein and telomerase components was evaluated in tissue biopsy specimens from patients with chronic hepatitis C, the expression of La protein strongly correlated with hTR. Moreover, it correlated significantly with the representative telomerase components p23 and HSP90 (Figure 6).

Repression of replication of JFH-1 in Huh-7.5 cells by recombinant adenovirus expressing short-hairpin RNA against La protein. Expression of La protein is induced by HCV infection, and it activates telomerase activity in Huh-7.5 cells. Therefore, it could be important to suppress La protein not only for the inhibition of HCV, but also for reducing the oncogenic potential of hepatocytes infected with HCV.

We constructed recombinant adenovirus expressing short-hairpin RNA against La protein (Ad-shLa). JFH-1 RNA was transfected into Huh-7.5 cells and 12 h after transfection, cells were exposed with Ad-shLa or control adenovirus (Ad-Null) for 1 h. At 12, 36, and 60 h after injection, changes in the levels of HCV RNA and La protein were evaluated by RTD-PCR and

Western blotting (Figure 7). At 60 h after injection, Ad-shLa repressed the level of La protein to 30% of that in the control cells (Figure 7*A*, 7*C*). Under these conditions, JFH-1 replication was significantly repressed to 50% at the RNA level (Figure 7*B*) and to 30% at the protein level (Figure 7*D*) of the control.

DISCUSSION

The translation machinery of HCV is simple and requires only the ribosomal 40s subunit, eIF2/GTP/Met-tRNA complex, and eIF3 to initiate translation [15]. However, many other canonical and noncanonical translation initiation factors interact with the HCV IRES and might regulate HCV translation [15]. However, the functional relevance of these factors for HCV replication has not yet been fully clarified.

Among 14 canonical and noncanonical translation initiation factors, we confirmed that La protein, PTB, eIF2γ, and PSMA7 had functional relevance for HCV IRES activity in RCF-26 cells. In the rabbit reticulocyte lysate, La protein, PTB, eIF3 p170, PCBP1, and PCBP2 significantly increased HCV IRES activity.

To evaluate the role of IRES activity in HCV replication, we constructed a translation incompetent infectious HCV clone, JFH-1 338U, by introducing a single-nucleotide mutation from A to U at nucleotide 338 in the 5′ nontranslated RNA that stabilized the stem-loop domain IV structure and impaired HCV translation, as reported elsewhere [12]. The La protein binds stem-loop IV, relaxes the stem-loop structure, and enhances HCV IRES activity [5].

Transfection of JFH-1 338U RNA into Huh-7.5 cells resulted in the production of neither HCV RNA nor HCV core protein. La protein overexpression could not overcome the replication defect by the 338U mutation (data not shown). These results indicate that JFH-1 338U was not only translation incompetent but also replication incompetent.

Interestingly, when the relationship between these initiation factors and HCV replication was investigated, we found that the initiation factors were induced by JFH-1 replication in Huh-7.5 cells. The relationship between these initiation factors and HCV replication was also evaluated in liver biopsy specimens from patients with chronic hepatitis C.

La protein has been reported to be one of the components of telomerase [14]; therefore, we evaluated the functional role of La protein on telomerase activity. Overexpression of La protein in Huh-7 cells increased telomerase activity significantly, as evaluated by the TRAP assay. The expression of hTR, an RNA template of human telomerase reverse transcriptase was increased. La protein could bind to the double-stranded RNA structure and possibly stabilize hTR. Importantly, JFH-1 infection activated telomerase activity and induced hTR in Huh-7.5 cells.

Interestingly, La protein significantly correlated with hTR, p23, and HSP90, representative telomerase components, in the tissue specimens from patients with chronic hepatitis C. Several reports have also shown a low but significant level of expression of human telomerase reverse transcriptase in regenerating hepatocytes in cirrhotic livers [16]. These hepatocytes could overcome cellular senescence and transform into tumor cells if the associated genetic or epigenetic changes occurred during the course of chronic hepatitis C infection.

In this study, we constructed recombinant adenovirus expressing short-hairpin RNA against La protein and successfully suppressed the replication of the infectious HCV clone JFH-1 for the first time, to our knowledge. The virological significance of La protein for HCV replication using infectious HCV clone has not been reported before to our knowledge [17].

Because La protein is essentially involved in HCV IRES activity, its production is induced by HCV itself, and it potentially activates telomerase activity, it might be an exceptionally good candidate therapeutic target. Additional research into the development of small molecules, such as small peptides and chemical compounds, that are active against La protein could be useful for the development of novel anti-HCV therapeutic agents.

Acknowledgments

We thank Mikiko Nakamura and Nami Nishiyama for excellent technical assistance. We also thank Professor C. M. Rice, of Rockefeller University, for kindly providing the Huh-7.5 cells.

References

1. Kiyosawa K, Sodeyama T, Tanaka E, et al. Interrelationship of blood transfusion, non-A, non-B hepatitis and hepatocellular carcinoma: analysis by detection of antibody to hepatitis C virus. Hepatology **1990**; 12: 671–675.
2. Fried MW, Shiffman ML, Reddy KR, et al. Peginterferon alfa-2a plus ribavirin for chronic hepatitis C virus infection. N Engl J Med **2002**; 347:975–982.
3. Hara H, Aizaki H, Matsuda M, et al. Involvement of creatine kinase B in hepatitis C virus genome replication through interaction with the viral NS4A protein. J Virol **2009**; 83:5137–5147.
4. Tsukiyama-Kohara K, Iizuka N, Kohara M, Nomoto A. Internal ribosome entry site within hepatitis C virus RNA. J Virol **1992**; 66: 1476–1483.
5. Ali N, Siddiqui A. The La antigen binds 5′ noncoding region of the hepatitis C virus RNA in the context of the initiator AUG codon and stimulates internal ribosome entry site-mediated translation. Proc Natl Acad Sci U S A **1997**; 94:2249–2254.
6. Ali N, Siddiqui A. Interaction of polypyrimidine tract-binding protein with the 5′ noncoding region of the hepatitis C virus RNA genome and its functional requirement in internal initiation of translation. J Virol **1995**; 69:6367–6375.
7. Honda M, Kaneko S, Matsushita E, Kobayashi K, Abell GA, Lemon SM. Cell cycle regulation of hepatitis C virus internal ribosomal entry site-directed translation. Gastroenterology **2000**; 118:152–162.
8. Honda M, Shimazaki T, Kaneko S. La protein is a potent regulator of replication of hepatitis C virus in patients with chronic hepatitis C through internal ribosomal entry site-directed translation. Gastroenterology **2005**; 128:449–462.
9. Shimazaki T, Honda M, Kaneko S, Kobayashi K. Inhibition of internal

ribosomal entry site-directed translation of HCV by recombinant IFN-α correlates with a reduced La protein. Hepatology **2002**; 35:199–208.
10. Honda M, Kaneko S, Kawai H, Shirota Y, Kobayashi K. Differential gene expression between chronic hepatitis B and C hepatic lesion. Gastroenterology **2001**; 120:955–966.
11. Wakita T, Pietschmann T, Kato T, et al. Production of infectious hepatitis C virus in tissue culture from a cloned viral genome. Nat Med **2005**; 11:791–796.
12. Honda M, Brown EA, Lemon SM. Stability of a stem-loop involving the initiator AUG controls the efficiency of internal initiation of translation on hepatitis C virus RNA. RNA **1996**; 2:955–968.
13. Forsythe HL, Jarvis JL, Turner JW, Elmore LW, Holt SE. Stable association of hsp90 and p23, but not hsp70, with active human telomerase. J Biol Chem **2001**; 276:15571–15574.
14. Ford LP, Shay JW, Wright WE. The La antigen associates with the human telomerase ribonucleoprotein and influences telomere length in vivo. RNA **2001**; 7:1068–1075.
15. Pestova TV, Shatsky IN, Fletcher SP, Jackson RJ, Hellen CU. A prokaryotic-like mode of cytoplasmic eukaryotic ribosome binding to the initiation codon during internal translation initiation of hepatitis C and classical swine fever virus RNAs. Genes Dev **1998**; 12:67–83.
16. Kawakami Y, Kitamoto M, Nakanishi T, et al. Immuno-histochemical detection of human telomerase reverse transcriptase in human liver tissues. Oncogene **2000**; 19:3888–3893.
17. Xue Q, Ding H, Liu M, et al. Inhibition of hepatitis C virus replication and expression by small interfering RNA targeting host cellular genes. Arch Virol **2007**; 152:955–962.

Published OnlineFirst May 18, 2010; DOI:10.1158/0008-5472.CAN-09-4210

Tumor and Stem Cell Biology

Cancer Research

Oncostatin M Renders Epithelial Cell Adhesion Molecule–Positive Liver Cancer Stem Cells Sensitive to 5-Fluorouracil by Inducing Hepatocytic Differentiation

Taro Yamashita, Masao Honda, Kouki Nio, Yasunari Nakamoto, Tatsuya Yamashita, Hiroyuki Takamura, Takashi Tani, Yoh Zen, and Shuichi Kaneko

Abstract

Recent evidence suggests that a certain type of hepatocellular carcinoma (HCC) is hierarchically organized by a subset of cells with stem cell features (cancer stem cells; CSC). Although normal stem cells and CSCs are considered to share similar self-renewal programs, it remains unclear whether differentiation programs are also maintained in CSCs and effectively used for tumor eradication. In this study, we investigated the effect of oncostatin M (OSM), an interleukin 6–related cytokine known to induce the differentiation of hepatoblasts into hepatocytes, on liver CSCs. OSM receptor expression was detected in the majority of epithelial cell adhesion molecule–positive ($EpCAM^+$) HCC with stem/progenitor cell features. OSM treatment resulted in the induction of hepatocytic differentiation of $EpCAM^+$ HCC cells by inducing signal transducer and activator of transcription 3 activation, as determined by a decrease in stemness-related gene expression, a decrease in EpCAM, α-fetoprotein and cytokeratin 19 protein expressions, and an increase in albumin protein expression. OSM-treated $EpCAM^+$ HCC cells showed enhanced cell proliferation with expansion of the EpCAM-negative non-CSC population. Noticeably, combination of OSM treatment with the chemotherapeutic agent 5-fluorouracil (5-FU), which eradicates EpCAM-negative non-CSCs, dramatically increased the number of apoptotic cells *in vitro* and suppressed tumor growth *in vivo* compared with either saline control, OSM, or 5-FU treatment alone. Taken together, our data suggest that OSM could be effectively used for the differentiation and active cell division of dormant $EpCAM^+$ liver CSCs, and the combination of OSM and conventional chemotherapy with 5-FU efficiently eliminates HCC by targeting both CSCs and non-CSCs. *Cancer Res; 70(11); 4687–97. ©2010 AACR.*

Introduction

It is widely accepted that cancer is a disease that develops from a normal cell with accumulated genetic/epigenetic changes. Although considered monoclonal in origin, cancer is composed of heterogeneous cellular populations. These heterogeneities are traditionally explained by the clonal evolution of cancer cells through a series of stochastic genetic events (clonal evolution model; ref. 1). In contrast, cancer cells are known to have the capabilities characteristic of stem cells with respect to self-renewal, limitless division, and generation of heterogeneous cell populations. Recent evidence suggests that tumor cells possess stem cell features (cancer stem cells; CSC) to self-renew and give rise to relatively differentiated cells through asymmetric division, and thereby form heterogeneous populations (CSC model; refs. 2, 3). Accumulating evidence supports the notion that CSCs could generate tumors more efficiently in immunodeficient mice than non-CSCs in the case of leukemia and various solid tumors (4–9), although the origin of CSCs is still a controversial issue.

Worldwide, hepatocellular carcinoma (HCC) is one of the most common malignancies with poor outcome (10). Recent evidence suggests that at least some HCCs are organized by liver CSCs in a hierarchical manner (11). Several markers have been identified as useful for the enrichment of liver CSCs, including side population fraction (12), CD133 (13), CD90 (14), and OV6 (15). We have recently used epithelial cell adhesion molecule (EpCAM) and α-fetoprotein (AFP) to identify novel prognostic HCC subtypes related to certain developmental stages of human liver lineages (16). Among these, EpCAM-positive ($^+$) AFP^+ HCC (hepatic stem cell–like HCC) is characterized by young onset of disease, activation of Wnt/β-catenin signaling, and poor prognosis. *EPCAM* is a target gene of Wnt/β-catenin signaling (17), and we previously identified that $EpCAM^+$ HCC cells from primary HCC

Authors' Affiliation: Center for Liver Diseases, Kanazawa University Hospital, Kanazawa, Ishikawa, Japan

Note: Supplementary data for this article are available at Cancer Research Online (http://cancerres.aacrjournals.org/).

Corresponding Authors: Taro Yamashita, Department of Gastroenterology, Kanazawa University Graduate School of Medical Science, 13-1 Takara-Machi, Kanazawa, Ishikawa 920-8641, Japan. Phone: 81-76-265-2851; Fax: 81-76-265-4250; E-mail: taroy@m-kanazawa.jp and Shuichi Kaneko, Center for Liver Diseases, Kanazawa University Hospital; Department of Gastroenterology, Kanazawa University Graduate School of Medical Science, 13-1 Takara-Machi, Kanazawa, Ishikawa 920-8641, Japan. Phone: 81-76-265-2230; Fax: 81-76-265-4250; E-mail: skaneko@m-kanazawa.jp.

doi: 10.1158/0008-5472.CAN-09-4210

Published OnlineFirst May 18, 2010; DOI:10.1158/0008-5472.CAN-09-4210

samples and cell lines have the features of CSCs, at least in the hepatic stem cell–like HCC subtype (18). Thus, EpCAM seems to be a potentially useful marker for the isolation of liver CSCs in hepatic stem cell–like HCC.

CSCs are considered to be resistant to chemotherapy and radiotherapy (19–21), which may be associated with the recurrence of the tumor after treatment. These findings have led to the proposal of "destemming" CSCs, to induce the differentiation of CSCs into non-CSCs or to eradicate CSCs by inhibiting the signaling pathway responsible for self-renewal (22). Recent studies support this proposal and suggest the utility of bone morphogenetic proteins, activated during embryogenesis and required for differentiation of neuronal stem cells, to induce differentiation of brain CSCs and facilitate brain tumor eradication (23, 24). However, it is still debatable whether simple differentiation of CSCs effectively eradicates tumors (25).

Oncostatin M (OSM), an interleukin (IL)-6–related cytokine produced by $CD45^+$ hematopoietic cells, is known to enhance hepatocytic differentiation of hepatoblasts by inducing the activation of the signal transducer and activator of transcription 3 (STAT3) pathway (26). Although OSM, IL-6, and leukemia-inhibitory factor share STAT3 signaling cascades, OSM is known to exploit the distinct hepatocytic differentiation signaling in an OSM receptor (OSMR)–specific manner (27). In this study, we hypothesized that OSM induces hepatocytic differentiation of liver CSCs through the OSMR signaling pathway. We examined OSMR expression and the effect of OSM in $EpCAM^+$ HCC in terms of hepatocytic differentiation and antitumor activities.

Materials and Methods

Clinical HCC specimens

A total of 107 HCC tissues and adjacent noncancerous liver tissues were obtained from patients who underwent hepatectomy for HCC treatment from 1999 to 2007 in Kanazawa University Hospital. These samples were formalin-fixed and paraffin-embedded, and used for immunohistochemistry. HCC and adjacent noncancerous liver tissues were histologically diagnosed by two pathologists. An additional fresh $EpCAM^+$ AFP^+ HCC sample was obtained from a surgically resected specimen and immediately used for the preparation of single-cell suspensions and xenotransplantation. All tissue acquisition procedures were approved by the Ethics Committee and the Institutional Review Board of Kanazawa University Hospital. All patients provided written informed consent.

Cell culture and reagents

HuH1 and HuH7 cells were cultured as previously described (18). A primary HCC tissue was dissected and digested in 1 μg/mL of type 4 collagenase (Sigma-Aldrich Japan K.K.) solution at 37°C for 15 to 30 minutes. Contaminated RBC were lysed with ammonium chloride solution (STEMCELL Technologies) on ice for 5 minutes. $CD45^+$ leukocytes and Annexin V^+ apoptotic cells were removed by autoMACS-pro cell separator and magnet beads (Miltenyi Biotec K.K.). EpCAM-positive and -negative cells were enriched by autoMACS-pro cell separator and CD326 (EpCAM) MicroBeads (Miltenyi Biotec K.K.). Recombinant OSM was purchased from R&D Systems, Inc. 5-Fluorouracil (5-FU) was obtained from Kyowa Kirin.

Quantitative reverse transcription-PCR analysis

Total RNA was extracted using TRIzol (Invitrogen) according to the instructions of the manufacturer. The expression of selected genes was determined in triplicate using the 7900 Sequence Detection System (Applied Biosystems). Each sample was normalized relative to β-actin expression. Probes used were *TACSTD1*, Hs00158980_m1; *AFP*, Hs00173490_m1; *KRT19*, Hs00761767_s1; *hTERT*, Hs00162669_m1; *Bmi1*, Hs00180411_m1; *POU5F1*, Hs00999632_g1; *CYP3A4*, Hs00430021_m1; *OSMR*, Hs00384278_m1; and *ACTB*, Hs99999903_m1 (Applied Biosystems).

Western blotting

Whole cell lysates were prepared using radioimmunoprecipitation assay lysis buffer as described previously (28). Rabbit polyclonal antibodies to STAT3 (Cell Signaling Technology, Inc.), rabbit polyclonal anti-OSMR antibodies H-200 (Santa Cruz Biotechnology), mouse monoclonal anti–phosphorylated STAT3 (Tyr^{705}) antibody (3E2; Cell Signaling Technology), and mouse monoclonal anti–β-actin antibody (Sigma-Aldrich) were used. Immune complexes were visualized by enhanced chemiluminescence (Amersham Biosciences, Corp.) as described by the manufacturer.

Immunohistochemistry and immunofluorescence analyses

Immunohistochemistry was performed using Envision+ kits (DAKO) according to the instructions of the manufacturer. Anti-EpCAM monoclonal antibody, VU-1D9 (Oncogene Research Products), was used for detecting EpCAM. Goat anti-OSMR polyclonal antibodies (C-20) were obtained from Santa Cruz Biotechnology. Mouse anti-CYP3A4 polyclonal antibodies (Abnova), mouse anti–cytokeratin (CK) 19 monoclonal antibody (DAKO), and mouse anti–Ki-67 monoclonal antibody MIB-1 (DAKO) were used for detecting CYP3A4, CK19, and Ki-67, respectively. Samples with >5% positive staining in a given area for a particular antibody were considered to be positive. For immunofluorescence analyses, anti-EpCAM antibody (Oncogene Research Products), anti-gp130ST antibodies (Santa Cruz Biotechnology), and anti–phosphorylated STAT3 (Tyr^{705}) antibody (3E2; Cell Signaling Technology) were used. Alexa 488 FITC-conjugated anti-mouse IgG or Alexa 568 Texas red–conjugated anti-goat/rabbit IgG (Molecular Probes) were used as secondary antibodies. Confocal fluorescence microscopic analysis was performed essentially as previously described (18).

Fluorescence-activated cell sorting analyses

Cultured cells were trypsinized, washed, and resuspended in HBSS (Lonza) supplemented with 1% HEPES and 2% fetal bovine serum (FBS). Cells were then incubated with FITC-conjugated anti-EpCAM monoclonal antibody Clone Ber-EP4 (DAKO) on ice for 30 minutes, and analyzed using